

Biotribocorrosion (tribo-electrochemical) characterization of anodized titanium biomaterial containing calcium and phosphorus before and after osteoblastic cell culture

H. P. Felgueiras,^{1,2} L. Castanheira,^{2,3} S. Changotade,¹ F. Poirier,¹ S. Oughlis,¹ M. Henriques,⁴ C. Chakar,⁵ N. Naaman,⁵ R. Younes,⁵ V. Migonney,¹ J. P. Celis,⁶ P. Ponthiaux,³ L. A. Rocha,² D. Lutomski¹

¹Université Paris 13 Sorbonne Paris Cité, CSPBAT UMR CNRS 7244, Laboratoire de Biomateriaux et Polymères de Spécialité LBPS, UFR SMBH, 74, rue Marcel Cachin, 93017 Bobigny, Paris, France

²University of Minho, CT2M, Centre for Mechanical and Materials Technologies, Campus de Azurém, 4800-058 Guimarães, Portugal

³École Centrale de Paris, LGPM, Laboratoire de Génie des Procédés et Matériaux, Grande Voie des Vignes, 92295 Châtenay-Malabry, Paris, France

⁴University of Minho, IBB, Institute for Biotechnology and Bioengineering, Centre of Biological Engineering, Campus de Gualtar, 4710-057 Braga, Portugal

⁵USJ, University Saint-Joseph, Faculty of Dentistry, Beirut, Lebanon

⁶Catholic University of Leuven, MTM, Department of Metallurgy and Materials Engineering, 3001 Heverlee, Belgium

Received 19 November 2013; revised 2 May 2014; accepted 5 June 2014

Published online 3 July 2014 in Wiley Online Library (wileyonlinelibrary.com). DOI: 10.1002/jbm.b.33236

Abstract: The purpose of this study was to investigate the relationship between the osteoblastic cells behavior and biotribocorrosion phenomena on bioactive titanium (Ti). Ti substrates submitted to bioactive anodic oxidation and etching treatments were cultured up to 28 days with MG63 osteoblast-like cells. Important parameters of *in vitro* bone-like tissue formation were assessed. Although no major differences were observed between the surfaces topography (both rough) and wettability (both hydrophobic), a significant increase in cell attachment and differentiation was detected on the anodized substrates as product of favorable surface morphology and chemical composition. Alkaline phosphatase production has increased (≈ 20 nmol/min/mg of protein) on the anodized materials, while phosphate concentration has reached the dou-

ble of the etched material and calcium production increased (over 20 $\mu\text{g}/\text{mL}$). The mechanical and biological stability of the anodic surfaces were also put to test through biotribocorrosion sliding solicitations, putting in evidence the resistance of the anodic layer and the cells capacity of regeneration after implant degradation. The Ti osteointegration abilities were also confirmed by the development of strong cell–biomaterial bonds at the interface, on both substrates. By combining the biological and mechanical results, the anodized Ti can be considered a viable option for dentistry. © 2014 Wiley Periodicals, Inc. *J Biomed Mater Res Part B: Appl Biomater*, 103B: 661–669, 2015.

Key Words: biotribocorrosion, titanium biomaterial, anodization, osteoblastic cells, wearing

How to cite this article: Felgueiras HP, Castanheira L, Changotade S, Poirier F, Oughlis S, Henriques M, Chakar C, Naaman N, Younes R, Migonney V, Celis JP, Ponthiaux P, Rocha LA, Lutomski D. 2015. Biotribocorrosion (tribo-electrochemical) characterization of anodized titanium biomaterial containing calcium and phosphorus before and after osteoblastic cell culture. *J Biomed Mater Res Part B* 2015;103B:661–669.

INTRODUCTION

The technological progress and advances that characterize our society have led to an outstanding improvement in the dental field, particularly with the development of biomaterials.¹ A successful implantation relies on their chemical, physical, and mechanical properties as well as on their ability to influence and define the cells behavior. Biomaterials should not induce an abnormal host response or suffer degradation when exposed to body fluids.^{2–4} These requirements are of extreme importance to a successful implantation.

Titanium (Ti) has been considered over the past few years as the “gold standard” for orthopedic and dental implants.¹ Ti reacts with water and air to produce a thin oxide layer on its surface that prevents corrosion and enables the material to interact and establish a connection with the surrounding tissue, without causing an undesirable response.^{5–8} Still, this spontaneously formed oxide layer is usually thin and heterogeneous, which hinders the implant attachment.^{9,10} Furthermore, the passive film possesses poor tribological properties, such as low wear rate or unstable

Correspondence to: D. Lutomski (e-mail: lutomski@smbh.univ-paris13.fr)

friction coefficient.¹¹ Hence, to overcome these limitations, thermal and electrochemical surface treatments are applied.

Thicker oxide layers improving tribological and corrosion properties and enhancing cell attraction can be produced, by controlling the surface morphology, topography, and composition.⁷ Although, different surface treatments are capable of such task, sand-blasting, plasma spray, or acid etching, to name a few, recent reports suggest anodization to be a preferred method to form rough, porous, and thick oxide films on Ti materials.¹²

As a simple and fast method, anodization has attracted much attention. This technique allows the formation of bioactive coatings through the incorporation of calcium and phosphorus onto the Ti surfaces,^{13,14} or to control the roughness or wettability of the oxide layer increasing its osteointegration and/or osteoconduction.^{15,16} The primary purpose for coating calcium/phosphorus or hydroxyapatite onto implantable materials is the rapid attraction of bone tissue/cells onto their surface, at early stages of interaction. Fini et al.¹³ demonstrated this property on Ti based materials. By studying the effect of anodized bioactive coatings (calcium/phosphorus) on the osteoblast-like cells early response, *in vivo* and *in vitro*, they were able to confirm the materials good cytocompatibility and morphological characteristics as well as their osteointegration abilities. Franco et al.¹⁴ using primary osteoblastic cells, derived from alveolar bone, tested a new anodized alkali treatment (calcium/phosphorus) on Ti substrates and corroborated Fini et al results. They showed an increased cellular activity from the proliferation phase to early differentiation of the osteoblastic cells, associated with an enhanced collagen production. Still, the mechanical stability of the anodic films on Ti substrates as product of the human body biological, chemical, and mechanical changes remains a challenge.

The friction, wear, abrasion, and corrosion sensed by dental implants as a result of cyclic micro-movements by way of mastication loads, sliding-wear bite forces, and corrosive body fluids (oral cavity constant changes in pH) may lead to the implant deterioration.^{17,18} Moreover, whether Ti is used in crowns or implants, a relative displacement between it and the adjacent material (gum, bone...) might occur. In consequence, organic and inorganic specimens can migrate to the available space and in combination with the synergistic effect of corrosion and wear develop a tribocorrosion system that may accelerate implant failure.¹⁹ As degradation of the outermost layer of the implant is a probable event, the capacity of cell regeneration in response to it and the resistance of the interface bone-biomaterial, a clear marker of the surface mechanical and biological stability and osteointegration abilities, are therefore of particular interest. Biotribocorrosion tests are a recent tool in this research field that takes into consideration these phenomena.¹⁷ Their ability to reproduce simultaneously the corrosion and wear conditions associated with the biological environment has become essential to mimic the cellular response during or after implantation.²⁰

The aim of this work was to evaluate the MG63 osteoblast-like cells interaction with Ti surfaces submitted to a bioactive anodic treatment. To assure the anodic layer

stability in contact with the biological surroundings, the osteoblastic cells early attachment and subsequent maturation were followed up to 28 days. The MG63 regenerative ability was observed through the effect of tribocorroded Ti surfaces on the early cell development, and the resistance of the biomaterial-cell bond (osteointegration) put to the test by means of extreme mechanical stimulation.

MATERIALS AND METHODS

Material preparation

Samples, 20 × 20 mm² in area and 2 mm in thickness, were cut from a Ti grade 2 plate (Goodfellow Cambridge Limited, England). The substrates were cleaned first in an ultrasonic bath with acetone for 3 min and second in a Kroll's reagent solution (2% HF, Sigma, and 10% HNO₃, Acros, in 88% H₂O) for 10 min. The resulting samples, identified as etched, were used as controls.

Anodic treatment with a calcium acetate (0.35 mol/L, Sigma) and β-glycerophosphate (0.04 mol/L, Sigma) electrolyte was applied to half of the etched samples for 1 min, at RT (bioactive coating). 300 V DC power source and a platinum leaf cathode were used. The resulting samples are identified as anodized and cleaned ultrasonically in propanol for 10 min followed by distilled water (d.H₂O) for 5 min.

Prior to cell culture, both anodized and etched substrates were sterilized in two steps: first to achieve the physiologic pH (pH = 7.4) and to eliminate surface impurities and second to adsorb proteins from the culture medium. The materials were washed with 1.5M sodium chloride (NaCl, Fisher), 0.15M NaCl, ultra pure water and phosphate buffered saline (PBS, Gibco), three times each. Finally, each Ti face was sterilized with UV light at 30 W for 15 min. They were left in a non-complete medium of Dulbecco's Modified Eagle Medium (DMEM, Gibco) for 24 h at 37°C and 5% of CO₂, and overnight in a complete medium of DMEM supplemented with 10% of fetal bovine serum (FBS, PAMTM) under equal conditions.

Surface characterization

Morphology, chemical composition, and topography.

Scanning electron microscopy (SEM, JEOL JSM—T220A Scanning Microscope) operating at 20 kV was used in the surfaces morphology studies. The materials were sonicated in a pure water bath (60°C) for 10 min and dried in a vacuum oven overnight, before observation. Their elemental composition was assessed with an energy dispersive x-ray spectrometer (EDS, INCA model 5785, Oxford System) incorporated into the SEM.

A white light interferometer (New-View 6300, Zygo, Middlefield, CT) was used to establish the surface topography. Both profile delineation (2D evaluation—2D graphics) and surface area (3D evaluation—3D models) evaluations were conducted. This is a non-contact optical profiling system that measures step heights (up to 0.1 nm) and surface roughness. The lateral resolution applied was 2.72 μm and the objective working distance was 9.3 mm. Four equally separated areas were analyzed and treated with a micro-roughness filter with a cut-off of 0.08 mm. A thin gold layer

was sputtered to increase the reflection of the anodic samples. The average results are reported as average roughness (Ra) and single roughness depth (Rz) for 2D and the corresponding values Sa and Sz for 3D.

Contact angle and surface free energy. The wettability of the etched and anodized to pure water (polar liquid); formamide (polar liquid, Sigma); and bromonaphthalene (apolar liquid, Sigma) was determined using a contact angle meter apparatus (OCA 15 Plus, Dataphysics). Two microliters drops were placed on the samples surface at RT. Eight seconds after contact, the angles measured. Four points per sample and liquid were retrieved. The surface free energy was determined using a set of equations previously described.²¹

Biological tests: cellular culture and expansion

MG63 osteoblast-like cells derived from human osteosarcoma (ATCC) were cultured in DMEM supplemented with 10% FBS, 1% penicillin-streptomycin (Gibco), and 1% fungizone (Gibco) at 37°C in an atmosphere of 5% CO₂. The culture was monitored every 24 h and the medium exchanged every 48 h. Cellular passages were conducted whenever the confluence was equal to 80%, using trypsin-EDTA (Gibco). For the totality of the biological test, 2×10^4 cells/mL were added to each substrate.

For the alkaline phosphatase and mineralization experiments, 0.05 mM L-ascorbic acid (Sigma) and 10 mM β -glycerophosphate (Sigma) were added to the complete culture medium, and applied to the cultures from day 1. This was done so the osteoblastic cells differentiation was possible.

Cell attachment, spreading, and morphology. After 0.5, 2, and 4 h of culture, the number, organization, shape, and size of the osteoblasts attached to the Ti surfaces were studied.

The number of cells was determined using a cell counter (Multisizer III—Coulter Counter Z2 Beckman). MG63 cells were detached with trypsin-EDTA and the suspension mixed with isoton (Beckman Coulter®) in a 0.1% (v/v) ratio. Their viability was assessed using the trypan blue exclusion test in a malassez counting chamber (PolyLab).

The cells structure and morphology were evaluated by fluorescent microscopy (ZEISS Axiolab, Germany). The medium was removed; the samples were washed three times with PBS; and fixated with 4% formaldehyde (Sigma) in medium for 45 min at 4°C. After, the materials were rinsed with a PBS/BSA 0.4% (v/w) (bovine serum albumin, SAFC) solution, permeabilized in 0.1% (v/v) triton X100 (Labosi) in PBS for 15 min, immersed in a new PBS/BSA 3% (v/w) solution for 30 min, and finally rinsed one more time with PBS/BSA 0.4% (v/w). The actin fibers of the MG63 cells were stained with phalloidin (FluoProbes™) at a 1/40 (v/v) in PBS, for 4 h, providing a general observation of the cells cytoskeleton. Before observation, all surfaces were washed twice with PBS. Pictures were taken using a digital camera (Olympus Camedia C-5050).

The cells area/size was analyzed using the Quantity One: 1D Analysis Software. Six images were used per culture time and sample type.

Early differentiation: alkaline phosphatase activity. The alkaline phosphatase (ALP) activity was evaluated from 7 to 28 days by following the transformation of *p*-nitrophenylphosphate into *p*-nitrophenol at 37°C. The ALP was separated from the cellular membrane using triton X100 for 1 h, under agitation. Five hundred microliters of the resultant cellular suspension were mixed with 500 μ L of *p*-nitrophenylphosphate substrate (Acros) at a concentration of 20 mM in 2-amino-2-methyl-propanol buffer and left for 30 min at 37°C. The enzymatic activity was measured with a spectrometer (Safas Xenius) and expressed in nmol of *p*-nitrophenol produced per min and per mg of protein.

Late differentiation: mineralization. The MG63 cells mineralization was studied after 28 days of culture. Two milliliters of trichloroacetic acid (TCA/d.H₂O 15% [w/v], Sigma) was added to each well and left for 1 h, under agitation. After that time, calcium detection was initialized: 10 μ L of the solution was recovered and combined with 1 mL of Arsenazo III (Sigma) (15 min). The calcium produced was measured by its absorbance at 650 nm and compared to a calcium chloride (CaCl₂) and TCA (15%, w/v) calibration curve from 50 to 1000 μ g/mL.

The remaining suspension was left for another 48 h under agitation for phosphate detection. One hundred microliters of the suspension was recovered and combined with 800 μ L of a solution containing 50% of acetone (Carlo-Erbra), 25% of sulfuric acid (Acros), 25% of 10 mM ammonium molybdate in d.H₂O, and with 80 μ L of citric acid (1M, Sigma). After 30 min at RT, the phosphate produced was measured by its absorbance at 355 nm using a spectrometer and compared to a di-sodium hydrogenophosphate (Na₂HPO₄) and TCA (15%, w/v) calibration curve from 10 to 200 μ g/mL.

Biotribological tests

Surface modification. To mimic possible tribological contacts that may occur on biomaterials during implantation or manipulation processes as mean of mastication loads, unidirectional sliding tests were performed in a "pin-on-disc" tribometer (Multispecimen-tester, FALEX-TETRA). This procedure consists in a frictional rotating movement of a pin (alumina sphere) against a stationary substrate, immersed in an electrolyte. The rotating speed applied was 100 rpm (7200 cycles) with a normal load of 0.8 N (258 MPa) and the electrolyte used was culture medium to approximate the test scenario to the biological environment. The rotation and load values were selected to generate a maximum Hertzian contact pressure on the surface. To avoid plastic deformation, the applied load was kept smaller than the yield strength of Ti (275 MPa).²² These repetitive cycles of concentrated load were performed to simulate degradation by way of intense mastication or strong sliding-wear bite forces, *in vitro*.

Cell culture after biotribocorrosion assays. Prior to cell culture, the tribocorroded Ti materials (etched and anodized) were sonicated in a pure water bath at 60°C and sterilized in an autoclave (SANO Clay, Wolf) at 120°C.

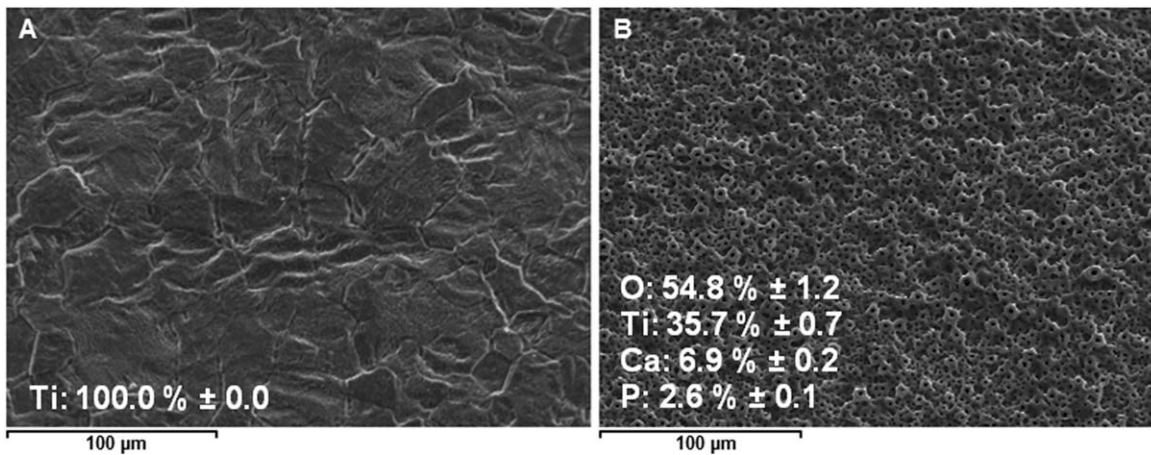


FIGURE 1. SEM micrographies of the (A) etched and (B) anodized surfaces morphology ($\times 500$ resolution) and respective chemical composition, expressed in mass percentage (Ti, titanium; O, oxygen; Ca, calcium; P, phosphorus).

2×10^4 cells/mL in complete medium were cultured onto these altered Ti substrates for 4 h, 3 and 7 days and the results were analyzed by SEM. In most cases, these periods correspond to cell attachment, early and advanced proliferation, respectively.

Tribocorrosion assays after cell mineralization. To test the bond strength at the interface MG63 osteoblastic cells—Ti materials and, simultaneously, validate the results from cell mineralization, unidirectional sliding tests were conducted after 28 days of culture (same conditions described in Surface Modification section). A complete medium supplemented with ascorbic acid and β -glycerophosphate was used. The results were observed by SEM.

Statistical analysis

Surface characterization tests were repeated three times while biological experiments were done six times, using two samples per group. Numerical data were reported as mean \pm standard deviation (SD). Statistical significance was determined by on-way analysis of variance (ANOVA) followed by the post hoc Bonferroni test, using the GraphPad Prism 5.0 software. Significance was defined as having $p < 0.05$.

RESULTS AND DISCUSSION

Surface characterization

The etched and anodized surfaces morphologies are shown in Figure 1. Although a rough and crimped structure is displayed by the etched substrates, in the anodized surfaces a

porous morphology prevails. This porosity resulted from the electrical discharges characteristics of the anodic treatment, a phenomenon also known as dielectric breakdown,^{1,6,12} and followed the original surface topography (etched waviness), as expected.⁶

Incorporation of calcium and phosphorus into the anodic oxide film was confirmed by EDS (Figure 1). As a result of consecutive oxidation and reduction reactions occurring during dielectric breakdown,¹ the compounds dissolved in the electrolyte, namely calcium acetate and β -glycerophosphate, were attracted to the anodic film conferring bioactive properties to the surface.^{23,24}

Despite a clear difference in morphologies, data retrieved from roughness measurements (Table I) turned out to be quite similar between the two substrates. Both displayed important levels of roughness consistent with previous work.²⁵ These similarities can be explained by the heterogeneity of the surface treatments. Although the anodic process was used to alter the surface composition but not the pore size and dispersion (these parameters were not controlled), the etching step was only applied to remove surface impurities. Therefore, irregular patterns on both surfaces can be assumed, which by consequence approximated their topographic results.

The surface hydrophobicity was assessed by contact angle measurements (Table II). The results show the anodized substrates to be the more hydrophobic from the group, although without statistical significance on the water contact angles. This is to be expected as increased roughness leads to higher contact angles.²⁶

TABLE I. 2D and 3D Topographic (Roughness) Evaluations of Etched and Anodized Titanium Surfaces Using White Light Interferometry

Method	Surface	2D Analyses		3D Analyses	
		Ra (μm)	Rz (μm)	Sa (μm)	Sz (μm)
Interferometry	Etched	0.98 ± 0.04	6.01 ± 0.41	0.98 ± 0.00	10.71 ± 0.42
	Anodized	1.00 ± 0.02	6.63 ± 0.32	1.02 ± 0.03	10.52 ± 0.74

TABLE II. Contact Angles of Water (θ_w), Formamide (θ_f), and Bromonaphthalene (θ_b) of the Etched and the Anodized Surfaces and Values of the Total Surface Energy (ΔG)

Surface	θ_w ($^\circ$)	θ_f ($^\circ$)	θ_b ($^\circ$)	ΔG (mJ/m ²)
Etched	92.20 \pm 2.98	93.34 \pm 1.26	28.87 \pm 4.21	-26.81
Anodized	98.74 \pm 3.19	94.08 \pm 2.08	53.27 \pm 1.10	-44.58

Biological tests

Cell attachment, spreading, and morphology. The number of MG63 cells attached to the surfaces as function of time is shown by Figure 2(A). The cells spreading and morphology for the same periods are given by Figure 2(B) and Figure 2(C), respectively. From the results, the anodic treatment enhances cell attachment from the very first moments of interaction,²⁷ while the etched surfaces are responsible for a superior cytoplasmatic cell spreading. Multiple researchers have reported that the surface roughness, morphology, and chemical composition affect the cellular behavior at early stages of development.^{14–16} It is well known, the presence of calcium and phosphorus ions on the oxide to favor greatly cell attachment. These free ions promote a physical and chemical bond with cells and, consequently, an environment compatible with osteogenesis.^{4,23} Besides, the probable presence of nanoporosity on the anodized substrates can strengthen the connection between cells and material and increase their adhesion rates.^{24,28} Regrettably, this irregular porosity can also be a challenge to cell spreading, hindering their cytoplas-

matic expansion,^{29,30} which explains the smaller sized MG63 cells observed on the anodized surfaces.

The osteoblastic cells morphology pattern [Figure 2(C)] was found equal for both Ti materials, with cells evolving from round to more elongated and polygonal shapes. After 30 min of contact, the majority of cells still displayed a spherical profile. Feng et al.²³ have shown that, at this point, cell adhesion is mainly based on chemical rather than physical interactions. After 2 h, a predominant heterogeneity in cells' shapes and sizes is obvious: while some are still round others exhibit a polygonal shape with small cytoplasmatic extensions. These cytoplasm projections are representative of the beginning of the physical contact and support the cells posterior evolution. At 4 h, almost 80% of the cells on both surfaces are well elongated (increased size), displaying the typical osteoblastic morphology. Because of the increased roughness and waviness of the surfaces, the orientation of the osteoblasts is not yet well defined. To the contrary, the cells cytoskeleton organization defined by the amount and extension of the actin fibers becomes more and more evident.

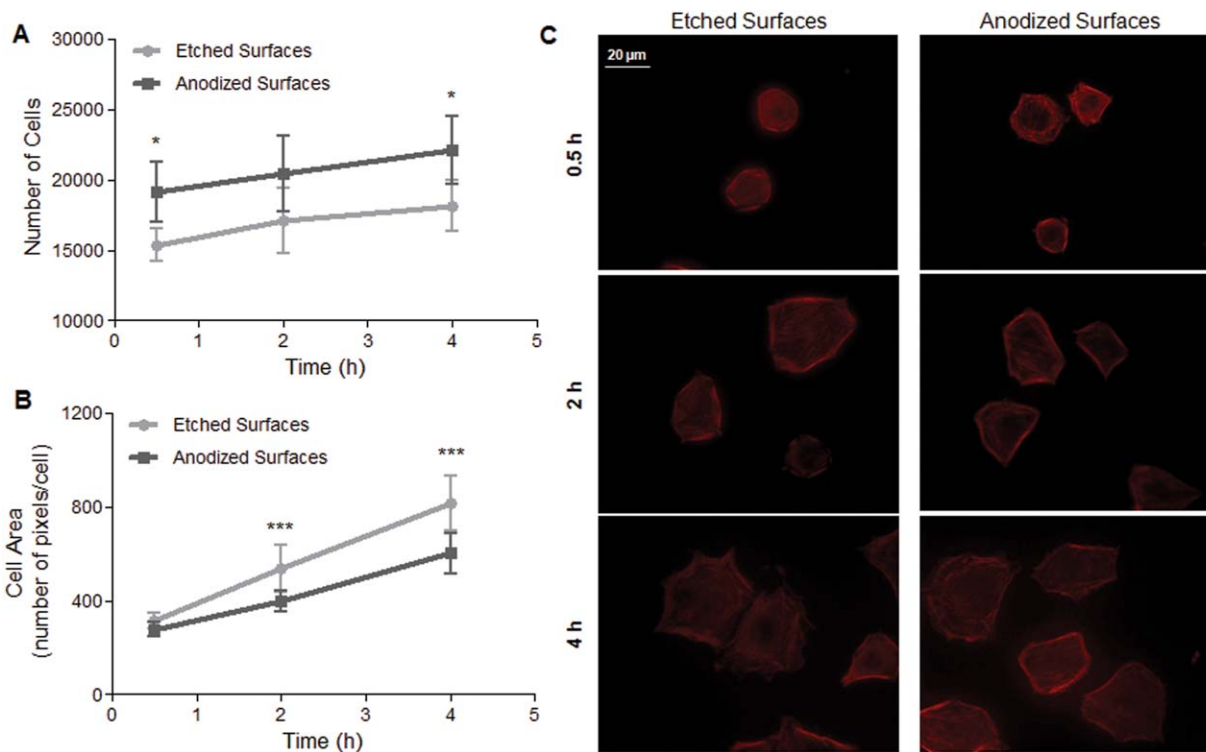


FIGURE 2. (A) Osteoblastic cells attachment on etched and anodized surfaces after 0.5, 2, and 4 h (significant differences are indicated by *, $p < 0.05$). (B) Fluorescent microscopy images (Phalloidin) of the MG63 cells morphology and geometry cultured on the etched and anodized substrates, from 0.5 to 4 h ($\times 40$ resolution), and respective (C) dimension (significant differences are indicated by ***, $p < 0.001$). [Color figure can be viewed in the online issue, which is available at wileyonlinelibrary.com.]

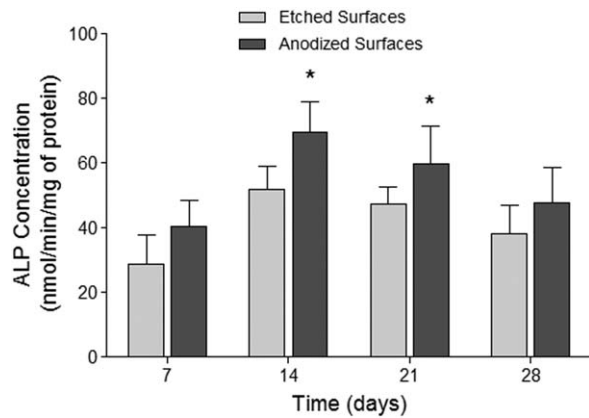


FIGURE 3. ALP produced by MG63 cells cultured from 7 to 28 days (significant differences are indicated by *, $p < 0.05$).

Cell differentiation. The ALP activity was followed for 28 days of culture, with the highest ALP production being registered at the 14th day, on both substrates (Figure 3). This maximum represents the highest cell metabolic activity and therefore the initial phase of the extracellular matrix (ECM) formation.³⁰ The ALP production was significantly enhanced by the anodized surfaces, which might suggest that the incorporated calcium and phosphorus accelerated the osteoblasts differentiation sequence most likely through a surface mediated mechanism.¹⁴ As expected, the ALP concentrations at 7 days were the lowest. This occurs because at the beginning of the MG63 cells development, proliferation is the

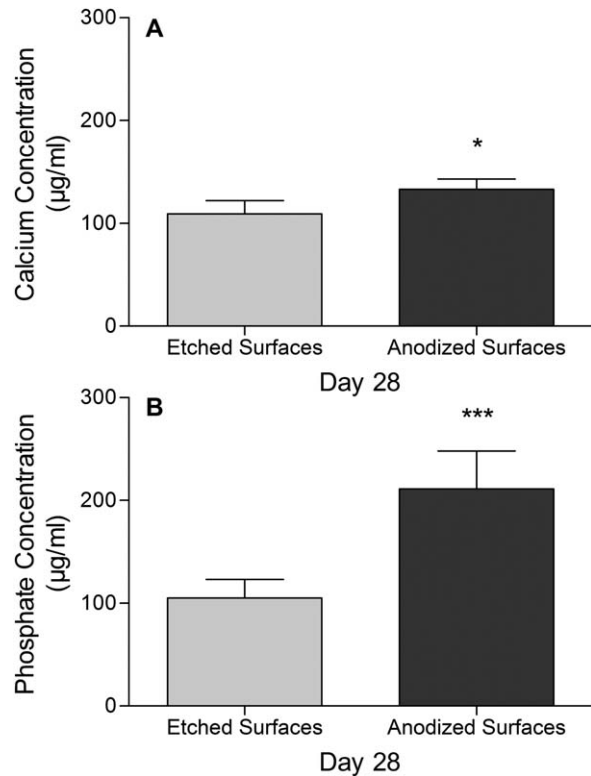


FIGURE 4. MG63 cells production of (A) calcium and (B) phosphate after 28 days of culture on etched and anodized surfaces.

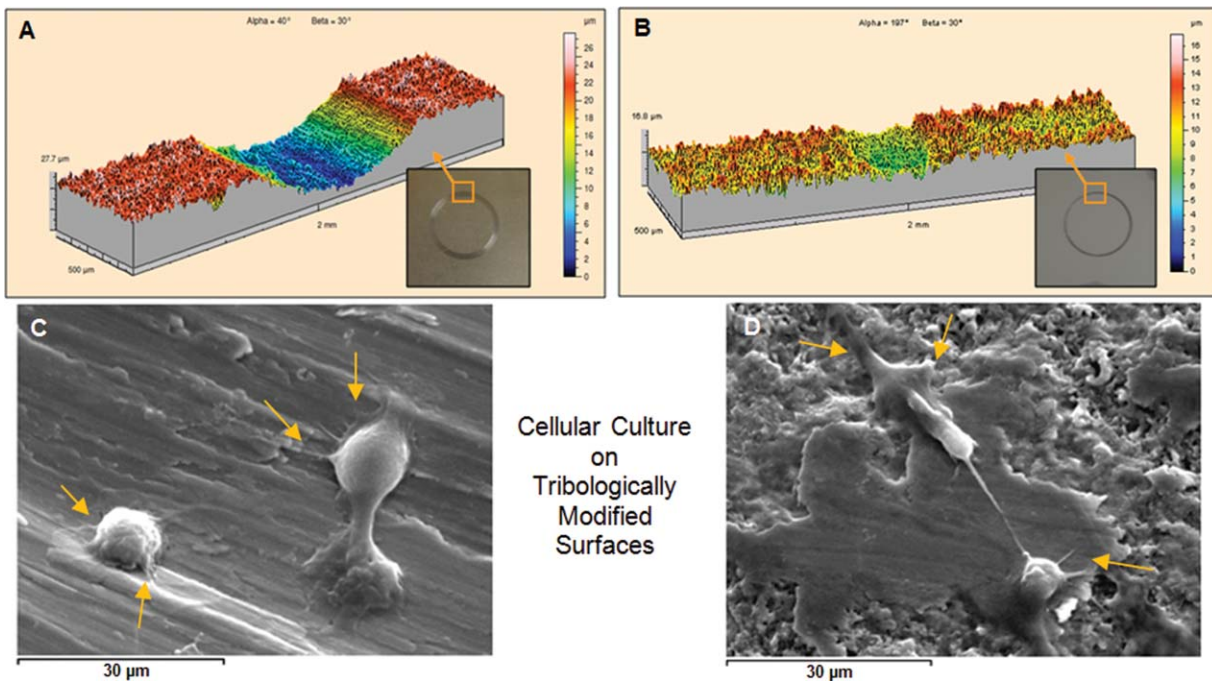


FIGURE 5. Real and 3D (microtopographies) aspect of the (A) etched and (B) anodized substrates after biotribocorrosion assays (load = 0.8 N). SEM microographies of the MG63 cells dispersion after 4 h of culture ($\times 2000$ resolution) on the (C) etched and (D) anodized wear track (center of the samples). Yellow arrows represent the osteoblastic cells tendency to extend protrusions to interact with rougher regions. [Color figure can be viewed in the online issue, which is available at wileyonlinelibrary.com.]

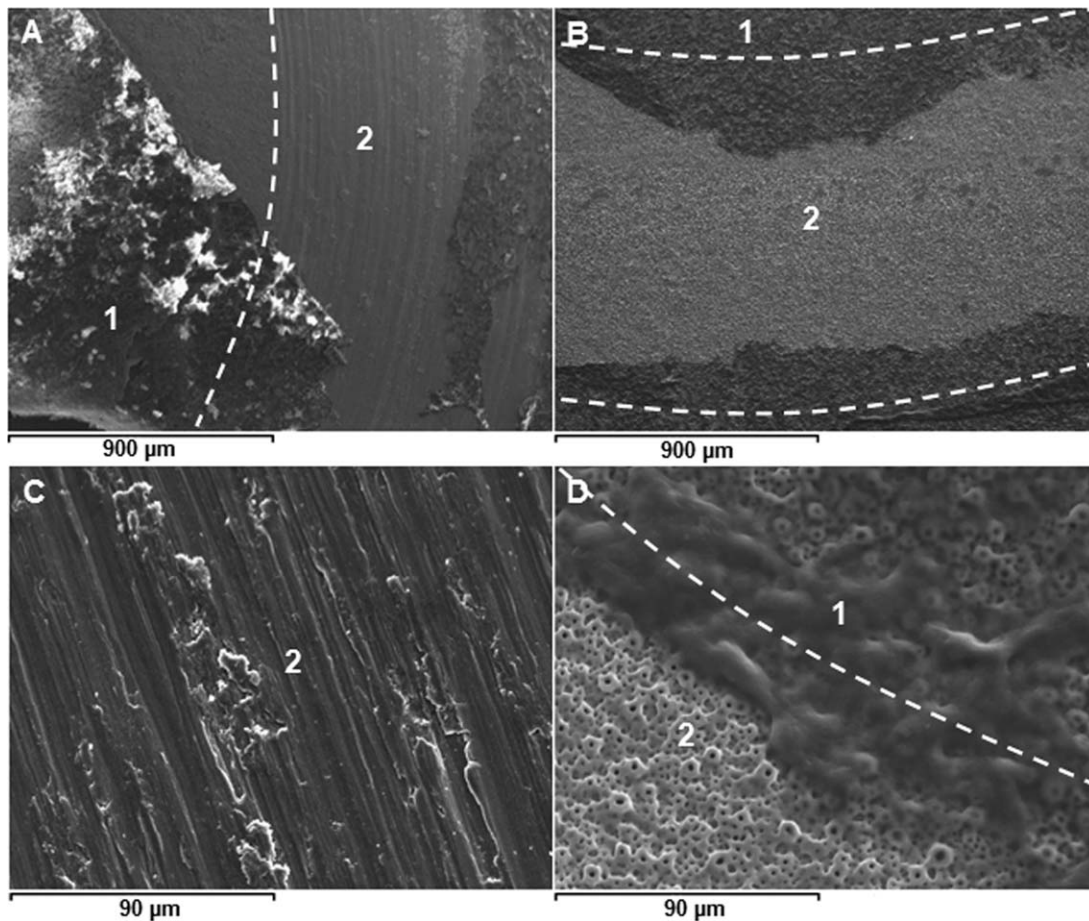


FIGURE 6. SEM micrographies representative of the biotribocorrosion (0.8 N) assays effect on (A) (C) etched and (B) (D) anodized surfaces cultured with MG63 cells for 28 days ($\times 75$ and $\times 750$ resolution, 1. Cellular Layer, 2. Wear Track).

dominant phase.³¹ It may be noted that, in this study, anodic treatment has no effect on cell proliferation (data not shown). After day 14, the ALP concentration decreases. This phenomenon is the outcome of the beginning of the second phase of osteoblastic cells differentiation, the ECM mineralization. ALP is an enzyme present in the cellular membrane capable of releasing phosphate ions to the ECM that interact with the pre-existing calcium ions, leading to the matrix mineralization.³⁰

The mineralization evaluations reported in terms of calcium and phosphate production were conducted for 28 days [Figure 4(A) and Figure 4(B), respectively]. Before that period, the expressions of calcium and phosphate ions were too insignificant to be considered (near to zero, data not shown). The results clearly point the ability of the anodized treatment to induce osteoblastic differentiation on titanium surfaces ($p < 0.05$), particularly the phosphate production ($p < 0.0001$). According to many authors,^{16,30,32,33} implantable surfaces enriched with calcium and phosphorus favor significantly the cells affinity to it and instigate their posterior maturation, especially in the presence of a supplemented culture medium (ascorbic acid and β -glycerophosphate). These additives display similar composition to the inorganic phase of bone (60%) and adopt a par-

titular osteoblastic phenotype expression when in the medium, triggering a series of molecular events that culminate in the cells differentiation.³³⁻³⁵ It has been also documented that rougher surfaces associated to these chemical elements can favor the ECM maturation.^{15,16}

Biotribological tests

Cellular culture after biotribocorrosion assays. The “pin-on-disc” biotribocorrosion tests applied to regular surfaces induced the formation of a wear track in the center of the etched and anodized materials [Figure 5(A,B)]. This experiment was conducted to assess the cells regenerative capacity after implant degradation, by means of implant screwing (during implantation) or mastication loads (after implantation). In simultaneous, the surfaces resistance to abrasion and corrosion was compared.

MG63 cells were culture for 4 h, 3 and 7 days on the tribologically altered surfaces. After 4 h, it was evident the cells cytoplasmatic protrusions (yellow arrows) tendency to be connected with rougher regions present along the wear track [Figure 5(C,D)]. It is plausible that MG63 cells developed those contact points to sustain the interfacial bond and support posterior cell development.^{12,36} On both surfaces, the osteoblasts exhibited two physical morphologies:

spherical on smooth regions, and flatted and well spread in the rougher areas.

With this assay, the ability of osteoblastic cells to interact with tribologically altered surfaces was confirmed. Initial attachment results (4 h) point to a slower interaction between cells and altered material than on regular substrates but a possible one. Proliferation rates from regular and altered substrates up to 7 days confirmed this fact (data not shown). At 7 days, the anodized Ti wear tracks were almost totally covered with cells, oriented from the regular to the tribocorroded surface areas (preference for the bioactive anodic film). The same orientation was seen on the etched materials. Still, the confluence was a lot smaller. This is consequence of the weaker abrasion resistance demonstrated by the etched Ti that led to the formation of a bigger and well defined sliding track with a smooth surface, undesirable for cellular establishment.^{12,37}

Tribocorrosion assays after cell culture onto biomaterial. To follow the resistance of the cell–biomaterial bond at the interface (osteointegration) and acquire information about the mechanical and biological stability of the anodic film, biotribocorrosion tests were conducted after cell culture. Complete medium was used as electrolyte to approach the experiment to possible real phenomena. By mimicking the biological environment, a probable scenario of strong mastication loads was created (extreme conditions), to compare the resistance of the osteoblastic cells connection with the etched and the anodized Ti after near a month of implantation (28 days).

At the 28th day of culture, the Ti samples were completely covered by a cellular layer. Based on the mineralization results, this layer should be strong and resistant to mechanical solicitation in the same way as the inorganic phase of bone.^{38–40} That conception was confirmed by the SEM images recovered. Figure 6(A,B) revealed the presence of biological material in the sliding track of both etched and anodized substrates, respectively, after the “pin-on-disc” tribological tests. These experiments were conducted under severe conditions where the bone–biomaterial system was submitted to strong and repetitive mechanical solicitations for a short period of time (analogy to extreme real phenomena, such as strong sliding-wear bites). Therefore, it can be concluded that the MG63 cells mineralization, for both cases, was in fact efficient and that a reliable interface was created.

Observations at larger scale of the sliding tracks [Figure 6(C,D)] provided new proof of the anodized surfaces wear resistance. Very little deformation was detected on the anodized materials after repetitive loading [Figure 6(D)], with a clear prevalence of its original porous morphology. In contrast, extended traces of sliding were found in the etched substrates [Figure 6(C)] reflecting their fragile condition.^{12,37} By combining this information with the biological results, it is suggested that at reduced load (normal real life conditions of mastication) the bond resistance between cells and biomaterial would be superior for the anodized Ti.

CONCLUSION

In this study, Ti materials were submitted to anodic treatment and their performance in contact with osteoblastic cells tested, *in vitro*.

It was found that anodic surfaces enriched with calcium and phosphorus enhance cell attachment and differentiation (ALP production and mineralization). To the contrary, it was the etched Ti that provided the most suitable conditions for cell spreading. Biotribocorrosion tests provided insightful information about the mechanical and biological stability of the anodic film, during and after implantation, demonstrating its superior resistance to repetitive sliding solicitation and its ability to induce cell attachment even after degradation. The strength of the bond biomaterials–cells was also verified, confirming a viable osteointegration, which may be enhanced by the anodized substrates under normal load conditions (real life mastication loads).

Considering the dentistry as one of the most useful applications of Ti and the oral cavity as one of the most hardest biological environments to implants, the anodic coating of Ti could be technically and economically viable alternative to obtain wear and corrosion resistant dental implants.

REFERENCES

1. Le Guehennec L, Soueidan A, Layrolle P, Amouriq Y. Surface treatments of titanium dental implants for rapid osseointegration. *Dent Mater* 2007;23:844–854.
2. Whitters CJ, Strang R, Brown D, Clarke RL, Curtis RV, Hatton PV, Ireland AJ, Lloyd CH, McCabe JF, Nicholson JW, Scrimgeour SN, Setcos JC, Sherriff M, van Noort R, Watts DC, Wood D. Dental materials: 1997 literature review. *J Dent* 1999;27:401–435.
3. Zhou ZR, Zeng J. Tribology of dental materials: A review. *J Phys D: Appl Phys* 2008;41:1–22.
4. Zhu ZR, Yang D, Ma F. Investigation of a new design for zirconia dental implants. *J Med Coll PLA* 2007;22:303–311.
5. Kasemo B, Lausma J. Metal selection and surface characteristics. In: Quintessence Publishing Co. I, editor. *Tissue-Integrated Prostheses: Osseointegration in Clinical Dentistry*; Quintessence Publishing, 1985. pp 99–116.
6. Kuromoto NK, Simao RA, Soares GA. Titanium oxide films produced on commercially pure titanium by anodic oxidation with different voltages. *Mater Charact* 2007;58:114–121.
7. Zhu X, Chen J, Scheideler L, Reichl R, Geis-Gerstorf J. Effects of topography and composition of titanium surface oxides on osteoblast responses. *Biomaterials* 2004;25:4087–4103.
8. Pourbaix M. *Atlas of Electrochemical Equilibria in Aqueous Solutions*, 2nd ed. USA: Nace TX; 1974.
9. Carlsson L, Rostlund T, Albrektsson B, Albrektsson T, Branemark PI. Osseointegration of titanium implants. *Acta Orthop Scand* 1986;57:285–289.
10. Branemark PI. Introduction to osseointegration. In: Quintessence Publishing Co. I, editor. *Tissue-Integrated Prostheses: Osseointegration in Clinical Dentistry*; Quintessence Publishing, 1985. pp 11–76.
11. Krishna DSR, Brama YL, Sun Y. Thick rutile layer on titanium for tribological applications. *Tribol Int* 2007;40:329–334.
12. Gabbi C, Cacchioli A, Ravanetti F, Spaggiari B, Borghetti P, Martini FM, et al. Osteogenesis and bone integration: The effect of new titanium surface treatments. *Ann Fac Medic Vet di Parma* 2005;25:307–318.
13. Fini M, Cigada A, Rondelli G, Chiesa R, Giardino R, Giavarsi G, et al. In vitro and in vivo behaviour of Ca- and P- enriched anodized titanium. *Biomaterials* 1999;20:1587–1594.
14. Franco RL, Chiesa R, Beloti MM, Oliveira PT, Rosa AL. Human osteoblastic cell response to Ca- and P- enriched titanium surface obtained by anodization. *J Biomed Mater Res A* 2009;88:841–848.

15. Frauchiger VM, Schlottig F, Gasser B, Textor M. Anodic plasma-chemical treatment of CP titanium surfaces for biomedical applications. *Biomaterials* 2004;25:593–606.
16. Das K, Bose S, Bandyopadhyay A. Surface modifications and cell-materials interactions with anodized Ti. *Acta Biomater* 2007;3:573–585.
17. Souza JC, Henriques M, Oliveira R, Teughels W, Celis JP, Rocha LA. Do oral biofilms influence the wear and corrosion behavior of titanium? *Biofouling* 2010;26:471–478.
18. Vieira A, Ribeiro A, Rocha L, Celis J-P. Influence of pH and corrosion inhibitors on the tribocorrosion of titanium in artificial saliva. *Wear* 2006;261:994–1001.
19. Souza J, Barbosa S, Ariza E, Celis J-P, Rocha L. Simultaneous degradation by corrosion and wear of titanium in artificial saliva containing fluorides. *Wear* 2012;292–293:82–88.
20. Squire MW, Ricci JL, Bizios R. Analysis of osteoblast mineral deposits on orthopaedic/dental implant metals. *Biomaterials* 1996;17:725–733.
21. Van Oss CJ, Ju L, Chaudhury MK. Estimation of the polar parameters of the surface tension of liquids by contact angle measurements on gels. *J Colloid Interface Sci* 1989;128:313–319.
22. Landolt D, Mischler S. Electrochemical methods in tribocorrosion: A critical appraisal. *Electrochim Acta* 2001;46:3913–3929.
23. Feng B, Weng J, Yang BC, Qu SX, Zhang XD. Characterization of titanium surfaces with calcium and phosphate and osteoblast adhesion. *Biomaterials* 2004;25:3421–3428.
24. Thirugnanam A, Kumar TSS, Chakkingal U. Bioactivity enhancement of commercial pure titanium by chemical treatments. *Trends Biomater Art Organs* 2009;23:76–85.
25. Alves SA, Bayón R, Igartua A, Saénz de Viteri V, Rocha LA. Tribocorrosion behavior of anodic titanium oxide films produced by plasma electrolytic oxidation for dental implants. *Lubrication Sci* 2013. doi:10.1002/lis.1234.
26. Lim YJ, Oshida Y. Initial contact angle measurements on variously treated dental/medical titanium materials. *Biomed Mater Eng* 2001;11:325–341.
27. Lee JM, Lee JI, Lim YJ. In vitro investigation of anodization and CaP deposited titanium surface using MG63 osteoblast-like cells. *Appl Surf Sci* 2010;256:3086–3092.
28. Mendonca G, Mendonca DB, Aragao FJ, Cooper LF. Advancing dental implant surface technology—From micron- to nanotopography. *Biomaterials* 2008;29:3822–3835.
29. Zhu X, Chen J, Scheideler L, Altebaeumer T, Geis-Gerstorfer J, Kern D. Cellular reactions of osteoblasts to micron- and submicron-scale porous structures of titanium surfaces. *Cells Tissues Organs* 2004;178:13–22.
30. Helary G, Noirclere F, Mayingi J, Migonney V. A new approach to graft bioactive polymer on titanium implants: Improvement of MG63 cell differentiation onto this coating. *Acta Biomater* 2009;5:124–133.
31. Martin JY, Dean DD, Cochran DL, Simpson J, Boyan BD, Schwartz Z. Proliferation, differentiation, and protein synthesis of human osteoblast-like cells (MG63) cultured on previously used titanium surfaces. *Clin Oral Implants Res* 1996;7:27–37.
32. Zhao G, Schwartz Z, Wieland M, Rupp F, Geis-Gerstorfer J, Cochran DL, et al. High surface energy enhances cell response to titanium substrate microstructure. *J Biomed Mater Res A* 2005;74:49–58.
33. Zhu X, Kim KH, Jeong Y. Anodic oxide films containing Ca and P of titanium biomaterial. *Biomaterials* 2001;22:2199–2206.
34. Higuchi C, Myoui A, Hashimoto N, Kurivama K, Yoshioka K, Yoshikawa H, Itoh K. Continuous inhibition of MAPK signalling promotes the early osteoblastic differentiation and mineralization of the extracellular matrix. *J Bone Miner Res* 2002;17:1785–1794.
35. Kim KH, Ramaswaswamy N. Electrochemical surface modification of titanium in dentistry. *Dental Mater J* 2009;28:20–36.
36. Larsson C, Thomsen P, Aronsson BO, Rodahl M, Lausmaa J, Kasemo B, et al. Bone response to surface-modified titanium implants: Studies on the early tissue response to machined and electropolished implants with different oxide thicknesses. *Biomaterials* 1996;17:605–616.
37. Rodriguez R, Kim K, Ong JL. In vitro osteoblast response to anodized titanium and anodized titanium followed by hydrothermal treatment. *J Biomed Mater Res A* 2003;65:352–358.
38. Craig RG, Powers JM. *Restorative Dental Materials*, 11th ed. USA: Mosby, Inc; 2002.
39. Deng H-W, Liu Y-Z. *Current Topics in Bone biology*. London: World Scientific Publishing; 2005.
40. Kutz M. *Biomedical Engineering and Design Handbook*, 2nd ed. USA: McGraw Hill; 2009.